Pergamon

Available online at www.sciencedirect.com
SCIENCE DIRECT®

Cement and Concrete Research 34 (2004) 781–788

CEMENT AND CONCRETE RESEARCH

Electron microscopy and phase analysis of fly ash from pressurized fluidized bed combustion

Hiroki Maenami[a,*], Norifumi Isu[a], Emile H. Ishida[a], Takeshi Mitsuda[b]

[a]Basic Research Center, INAX Corporation, 3-77 Minatomachi, Tokoname, Aichi 479-8588, Japan
[b]Graduate School of Science and Engineering, University of East-Asia, Shimonoseki, Yamaguchi 751-8503, Japan

Received 18 December 2002; accepted 11 August 2003

Abstract

The characterization of the typical fly ashes from pressurized fluidized bed combustion system (PFBC) in Japan and Europe was carried out by electron microscopy and phase analysis using energy-dispersive X-ray spectroscopy (EDX). The purity of limestone as in-bed sulfur removal sorbent influences the desulfurization reaction. The high-purity limestone yielded both hydroxyl ellestadite and anhydrite in Japanese PFBC ashes, while dolomite-rich limestone yielded anhydrite in European PFBC ashes. When the high-purity limestone was used, hydroxyl ellestadite particles were observed as the independent particles or the rim around limestone particles. The Al_2O_3 content in the glassy phase was inversely proportional to the CaO content in the glassy phase, suggesting that the glassy phases were formed from metakaoline and calcite as end members. Since hydroxyl ellestadite, glassy phase and metakaoline are reactive under hydrothermal conditions, PFBC ashes are expected to be used as raw materials for autoclaved products.

Keywords: Fly ash; Characterization; SEM; EDX; Backscattered electron imaging

---

1. Introduction

Coal has attracted attention as a source of energy in the thermal power generation because of the relative abundance of deposit and exhaustion of fossil fuels. Since pressurized fluidized bed combustion (PFBC) system is an attractive technology for coal utilization due to the potential of a higher electricity efficiency of combined cycle plant [1], the amount of fly ash from PFBC (PFBC ash) will be increased in the near future. In Japan, three commercial PFBC power plants have been operated at Tomatou-Atsuma (85 MW, Hokkaido Electric Power), Osaki (250 MW, Chugoku Electric Power) and Karita (360 MW, Kyushu Electric Power) [2]. In Osaki plant, an additional 250-MW PFBC power unit is scheduled for construction by 2005. In Europe, three commercial PFBC power plants have been operated at Värtan (135 MW, Birka Energi, Sweden), Escatron (80 MW, Endesa, Spain) and Cottbus (76 MW, Stadwerke-Cottbus Kommunalfinanz Gruppe, Germany).

The PFBC ash contains higher amount of $CaCO_3$ and $CaSO_4$ because limestone ($CaCO_3$) is added as the in-bed sulfur removal sorbent at relatively low temperature (approximately 860 °C) and high pressure (approximately 1 MPa). The PFBC ash is different from the conventional fly ash generated at the pulverized coal firing system in that PFBC ash has much crystalline phases, less spherical glassy particles and lower CaO content.

However, in previous studies, the PFBC ash have been mainly characterized by mineral assemblage using X-ray diffraction (XRD) and chemical composition [3,4], and there are few reports about microscopic and mineralogical approaches for each mineral in PFBC ash. These microscopic and mineralogical approaches are important to clarify the mechanisms of desulfurization process by limestone, for a plant design and operating condition. In addition, they are also very important for utilization of PFBC ashes as raw materials of secondary cementitious products because the reaction and strength of products using the hydrothermal technology were strongly influ-

---

* Corresponding author. Tel.: +81-569-43-4866; fax: +81-569-43-4883.

E-mail address: maenami@i2.inax.co.jp (H. Maenami).

0008-8846/$ – see front matter © 2004 Published by Elsevier Ltd.
doi:10.1016/j.cemconres.2003.08.011

enced by the type of phases in raw materials, such as crystal or amorphous phases [5–7].

In this paper, using typical PFBC ashes from Japan and Europe, the electron microscopy and phase analysis by energy-dispersive X-ray spectroscopy (EDX) was carried out for the microscopic and mineralogical characterization of each mineral in PFBC ash.

2. Experimental

2.1. Samples

Four cyclone ashes from Ube PFBC test plant (4 MW, Chugoku Electric Power, Japan), Wakamatsu PFBC test plant (71 MW, Electric Power Development, Japan), Tomatou-Atsuma PFBC power plant and Karita PFBC power plant were used as Japanese PFBC ash. Two cyclone ashes from Värtan PFBC power plant and Cottbus PFBC power plant were used as European PFBC ash.

2.2. Analytical methods

The chemical composition, mineral assemblage and mean particle diameter of all samples were analyzed by X-ray fluorescence spectrometry (XRF; RIX3100, Rigaku, Japan), XRD (RAD-B, Rigaku, Japan) and laser scattering particle size distribution analyzer (LA-500, Horiba, Japan), respectively. The electron microscopy by field emission scanning electron microscope (FE-SEM: S-4700, Hitachi, Japan) and the phase analysis by EDX analyzer (EMAX-550, Horiba, Japan) were carried out. In the FE-SEM observation, the samples were implanted in epoxy resin and the polished surfaces were observed by backscattered electron imaging. Glassy phase in PFBC ash was identified by the polarization microscopy.

Table 1
Chemical composition, mineral assemblage and mean particle diameter of PFBC ashes from the Ube, Wakamatsu, Tomatou-Atsuma, Karita, Värtan and Cottbus plants

	Ube	Wakamatsu	Tomatou-Atsuma	Karita	Värtan	Cottbus
Chemical compositions (mass%)						
SiO_2	40	46	43	34	24	22
Al_2O_3	15	24	13	18	15	4.5
Fe_2O_3	1.1	2.4	1.9	1.9	6.2	12
CaO	29	16	31	29	24	29
MgO	0.4	0.5	0.7	4.5	16	14
K_2O	1.4	0.2	0.7	tr.	1.2	0.3
Na_2O	tr.	tr.	0.5	tr.	0.7	tr.
TiO_2	1.1	1.8	0.8	1.3	0.9	0.2
SrO	n.d.	n.d.	n.d.	tr.	n.d.	0.2
MnO	n.d.	n.d.	n.d.	n.d.	0.3	0.3
SO_3	6.0	6.9	4.2	3.5	4.8	12
P_2O_5	n.d.	0.3	n.d.	0.2	0.8	n.d.
L.O.I.	5.7	1.9	4.7	8.1	6.7	5.2
Mineral assemblage[a]						
	quartz (SiO_2)	quartz (SiO_2)	quartz (SiO_2)	quartz (SiO_2)	quartz (SiO_2)	quartz (SiO_2)
	hydroxyl ellestadite ($Ca_{10}(SiO_4)_3(SO_4)_3(OH)_2$)	anhydrite ($CaSO_4$)	lime (CaO)	calcite ($CaCO_3$)	anhydrite ($CaSO_4$)	anhydrite ($CaSO_4$)
	anhydrite ($CaSO_4$)	hydroxyl ellestadite ($Ca_{10}(SiO_4)_3(SO_4)_3(OH)_2$)	hydroxyl ellestadite ($Ca_{10}(SiO_4)_3(SO_4)_3(OH)_2$)	anhydrite ($CaSO_4$)	periclase (MgO)	dolomite ($CaMg(CO_3)_2$)
	calcite ($CaCO_3$)	anorthite ($CaAl_2Si_2O_8$)	anhydrite ($CaSO_4$)	hydroxyl ellestadite ($Ca_{10}(SiO_4)_3(SO_4)_3(OH)_2$)	calcite ($CaCO_3$)	periclase (MgO)
	lime (CaO)	mullite ($Al_6Si_2O_{13}$)	wollastonite ($CaSiO_3$)	lime (CaO)	anorthite ($CaAl_2Si_2O_8$)	calcite ($CaCO_3$)
	anorthite ($CaAl_2Si_2O_8$)	hematite (Fe_2O_3)	calcite ($CaCO_3$)	periclase (MgO)	lime (CaO)	$CaFe_2O_4$
	portlandite ($Ca(OH)_2$)	calcite ($CaCO_3$)	anorthite ($CaAl_2Si_2O_8$)	anorthite ($CaAl_2Si_2O_8$)	goethite (FeO(OH))	orthochrysotile ($Mg_3Si_2O_5(OH)_4$)
	wollastonite ($CaSiO_3$)		portlandite ($Ca(OH)_2$)	mullite ($Al_6Si_2O_{13}$)	hematite (Fe_2O_3)	larnite (Ca_2SiO_4)
			mullite ($Al_6Si_2O_{13}$)	dolomite ($CaMg(CO_3)_2$)		hematite (Fe_2O_3)
				magnesite ($MgCO_3$)		lime (CaO)
				gehlenite ($Ca_2Al_2SiO_7$)		orthoclase ($KAlSi_3O_8$)
				portlandite ($Ca(OH)_2$)		
Mean particle diameter (μm)						
	31.1	12.9	21.8	22.5	22.7	14.9

tr. = trace element; n.d. = not detected element. From top to bottom, the phases having higher intensity of XRD peaks are listed.

[a] Measured by XRD.

3. Results and discussion

3.1. Characteristics of PFBC ashes

Table 1 shows the chemical composition, mineral assemblage and mean particle diameter of the PFBC ashes from the Ube, Wakamatsu, Tomatou-Atsuma, Karita, Värtan and Cottbus plants. In the chemical compositions, the PFBC ashes have 16–31% CaO resulting from the addition of in-bed sulfur removal sorbent. The PFBC ashes from the Ube, Wakamatsu and Tomatou-Atsuma plants contain less than 1% MgO, the ash from Karita plant contains 4.5% MgO, and the ashes from Värtan and Cottbus plants contain about 15% MgO. These MgO contents reflect the chemical composition of limestone used as the sorbent. Relatively high-purity limestone is used in Japan, while dolomite-rich limestone is used in Europe. It is known that the amount of sulfur removal sorbent has to increase when dolomite-rich limestone is used because of the low desulfurization property [3,8]. Therefore, PFBC ashes from the Värtan and Cottbus plants have higher CaO and MgO and lower SiO_2 and Al_2O_3 than other PFBC ashes. This difference of the chemical composition is caused by the amount of the limestone added as a sorbent.

The PFBC ashes have also higher content of SO_3 from sulfur in the coal. The PFBC ash from Cottbus has the highest content of SO_3 (12 mass%) because the SO_3-rich brown coal is used.

Quartz, anhydrite, hydroxyl ellestadite, calcite, lime, periclase and dolomite were observed as main minerals in PFBC ashes. All PFBC ashes have quartz from the impurity of coal and limestone. Anhydrite and hydroxyl ellestadite were formed through the desulfurization reaction in the fluidized bed. Hydroxyl ellestadite was observed in the PFBC ashes with relatively low MgO content in Ube, Wakamatsu, Tomatou-Atsuma and Karita PFBC ashes. It can be presumed that the MgO content in the limestone influenced the formation of hydroxyl ellestadite, although a further investigation would be necessary. Calcite, lime, periclase and dolomite are residues in limestone as sulfur removal sorbent. Anorthite, mullite, wollastonite, gehlenite and larnite may be formed by the reaction in fluidized bed at high temperature.

The mean particle diameter of the PFBC ashes varied between 12.9 and 31.1 μm. These particle size distribution are influenced by the design and the operating conditions of a cyclone-collected PFBC ashes.

3.2. Microstructural observation of PFBC ashes

3.2.1. Desulfurization reaction

The XRD results showed that the PFBC ashes included anhydrite and hydroxyl ellestadite formed through the desulfurization reaction in the fluidized bed. In this section, the morphology of the products formed in desulfurization reaction and the mechanism of desulfurization reaction will be discussed.

FE-SEM observation showed that hydroxyl ellestadite particles existed in PFBC ashes as the independent particles (Fig. 1) or the rim of limestone particles (Fig. 2). One could suggest that the hydroxyl ellestadite was formed as rims on limestone particles and after this it separated as independent particles because of the exfoliation during the hard agitation in the fluidized bed. Under high magnification, it was observed that hydroxyl ellestadite was mingled with anhydrite in the size of several micrometers (Fig. 3).

The mechanisms of formation of anhydrite and hydroxyl ellestadite will be discussed. Generally, it is known that the

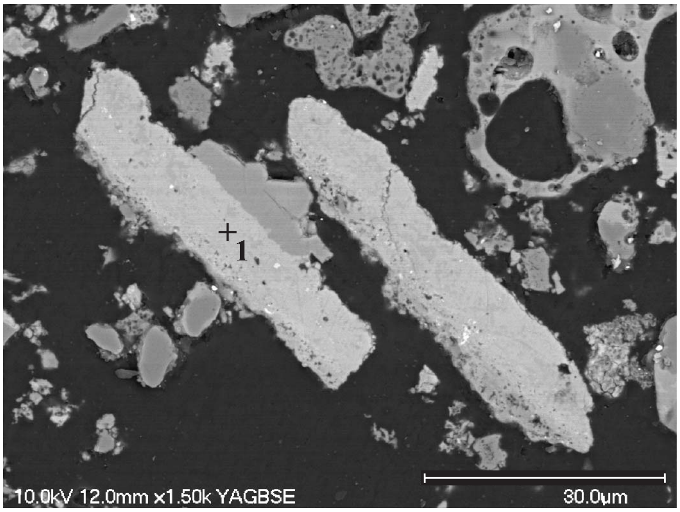

analysis point	1
SiO_2	19.2
Al_2O_3	6.5
CaO	50.8
SO_3	23.5

(mass%)

1: hydroxyl ellestadite

Fig. 1. SEM photograph and EDX results for hydroxyl ellestadite particles in the PFBC ash from Ube.

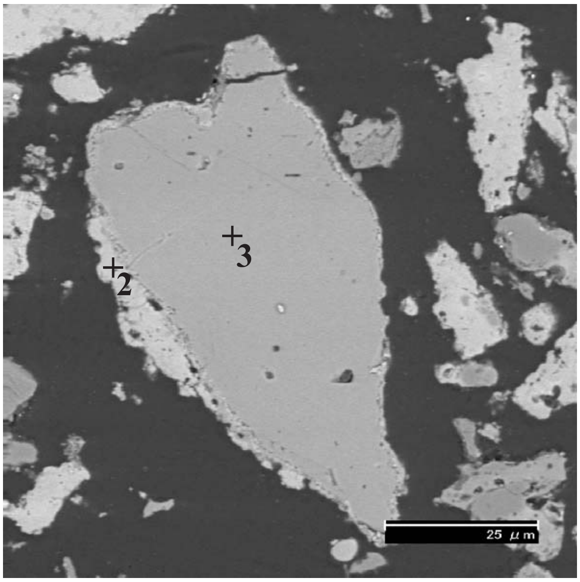

analysis point	2	3
SiO_2	16.9	-
Al_2O_3	3.2	-
CaO	55.4	100
SO_3	24.5	-

(mass%)

2: hydroxyl ellestadite
3: calcite

Fig. 2. SEM photograph and EDX results for a rim and a limestone particle in the PFBC ash from Ube.

desulfurization reaction in PFBC system proceeds according to the following reaction [3,8,9]:

$$CaCO_3 + SO_2 + 1/2O_2 \rightarrow CaSO_4 + CO_2$$

It has been suggested that $CaCO_3$ reacts directly with SO_x without the calcination of $CaCO_3$. The anhydrite is formed through this reaction. As it has been reported, hydroxyl ellestadite forms as a coproduct in cement kiln [10,11], therefore the hydroxyl ellestadite can be formed in fluidized bed at approximately 860 °C. In the fluidized bed, H_2O gas mainly comes from the water to make slurry mixed with the crushed coal and sorbent. The crushed coal and sorbent are fed by air pressure without water in the Tomatou-Atsuma PFBC plant. H_2O gas is also generated by dehydration of hydrous minerals such as clay which occur as impurities of coal and sorbent. It is observed that the glass and quartz adhere to the surface of limestone (Fig. 4). These results suggest that the hydroxyl ellestadite can be formed by the reaction among the anhydrite or limestone, glass, quartz, SO_x and H_2O gas in the fluidized bed.

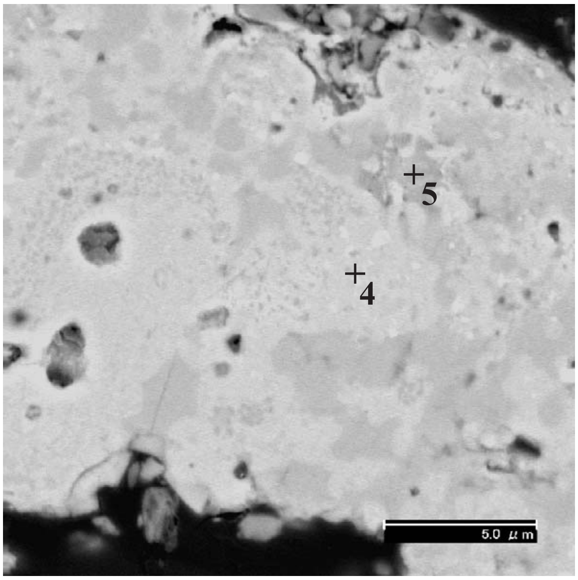

analysis point	4	5
SiO_2	15.9	6.4
Al_2O_3	11.9	0.5
CaO	52.5	43.3
SO_3	19.0	49.9
Cl	0.7	-

(mass%)

4: hydroxyl ellestadite
5: anhydrite

Fig. 3. SEM photograph and EDX results for hydroxyl ellestadite and anhydrite in the PFBC ash from Wakamatsu.

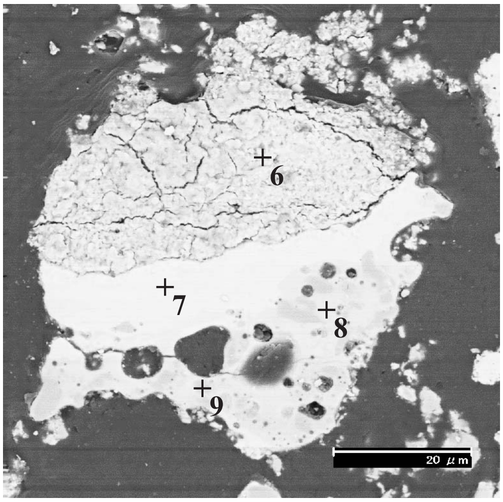

analysis point	6	7	8	9
SiO_2	7.0	49.2	56.4	97.4
Al_2O_3	2.7	9.0	18.7	-
CaO	87.2	40.7	20.6	-
MgO	1.2	0.4	-	-
Na_2O	0.2	-	0.5	0.7
K_2O	-	-	1.8	-
TiO_2	-	-	1.3	-
SO_3	1.2	0.7	0.7	-
Cl	0.5	-	-	1.9

(mass%)

6: calcite
7: glassy phase
8: glassy phase
9: quartz

Fig. 4. SEM photograph and EDX results for glass and quartz phases adhered to limestone particle in the PFBC ash from Ube.

On the other hand, when the dolomite-rich limestone is used as the sorbent, the anhydrite is formed on the surface of the dolomite particle, and the layer with the thickness of around 2 μm having lower SO_3 content is observed in the dolomite particle (Fig. 5). Many small pores are also observed in dolomite particles. It is considered that these pores have been formed by the decomposition of $MgCO_3$ because it is known that $MgCO_3$ in the dolomite is only decomposed under PFBC condition and the half-decomposed dolomite ($CaCO_3 \cdot MgO$) acts as the sorbent [3,8]. Hydroxyl ellestadite does not form when the dolomite-rich limestone is used as the sorbent. It is considered that the formation of hydroxyl ellestadite is influenced by MgO content in limestone, although a further investigation is necessary to elucidate the mechanism.

3.2.2. Formation of glassy phase

The glassy phase was observed by the polarization microscopy and FE-SEM with EDX in PFBC ashes. It was observed that the glassy phase was produced in reaction between metakaoline, quartz and calcite (Figs. 4, 6 and 7). The glassy phases were characterized by the spherical air bubbles and contained SiO_2, Al_2O_3 and CaO as major elements. Fig. 8 shows the relationship between Al_2O_3 and CaO concentration, as analyzed by EDX in glassy phase from different sources. The Al_2O_3 concentration of the glassy phase is inversely proportional to the CaO content of the glassy phase. This suggests the presence of two “end members” with higher amount of CaO and Al_2O_3, and that the glassy phases were formed as the mixture of two phases. The end members of the composition of glassy phase corresponded to the compo-

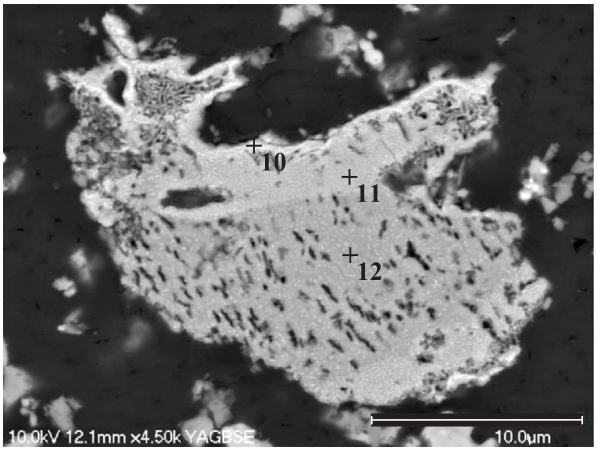

analysis point	10	11	12
SiO_2	0.7	0.4	0.8
Al_2O_3	0.3	-	0.5
Fe_2O_3	13.1	14.4	6.1
CaO	34.2	54.5	52.4
MgO	18.9	24.7	37.6
SO_3	33.0	4.0	-

(mass%)

10: anhydrite + dolomite
11: dolomite + anhydrite?
12: dolomite

Fig. 5. SEM photograph and EDX results for a dolomite particle in the PFBC ash from Värtan.

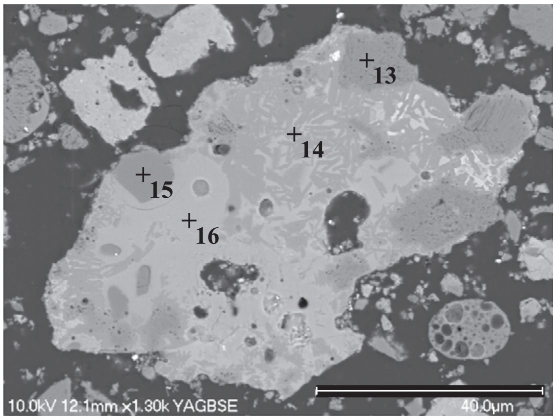

analysis point	13	14	15	16
SiO_2	52.7	46.9	56.6	51.9
Al_2O_3	45.5	35.0	17.7	14.5
CaO	-	17.7	19.1	27.1
Na_2O	0.7	0.4	-	0.1
K_2O	0.5	-	-	-
TiO_2	-	-	1.5	2.3
SO_3	0.6	-	5.2	4.2

(mass%)

13: metakaoline
14: anorthite
15: glassy phase
16: glassy phase

Fig. 6. SEM photograph and EDX results for metakaoline, anorthite and glassy phase in the PFBC ash from Wakamatsu.

sition of calcite and kaolinite shown in Fig. 8. Anorthite was crystallized from the glassy phase with similar composition (Fig. 6).

3.3. Possibility of utilization of PFBC ash for raw materials of the secondary product using the hydrothermal reaction

When the PFBC ashes are used as raw materials in hydrothermal technology, it is expected that the dissolution rate under hydrothermal conditions is strongly influenced by the type of components such as glassy phase or quartz, etc., besides the particle size [5–7].

When the PFBC ashes are used as raw materials of hydrothermal technology, quartz from PFBC ashes can yield the formation of tobermorite, the typical bonding material in hydrothermal products.

As it has been mentioned above, the hydroxyl ellestadite occurs in Japanese PFBC ashes. Sakiyama et al. [12] reported that the hydroxyl ellestadite is formed as the intermediate phase when the gypsum is added to the raw mixture on the producing process of lime–quartz based autoclaved board, and the presence of hydroxyl ellestadite strongly affects the high crystallinity of tobermorite. By using of the PFBC ashes with hydroxyl ellestadite as raw material, one can expect that the strength and the stability of volume in case of carbonation will be improved by the formation of highly crystalline tobermorite.

Furthermore, the amorphous phases in PFBC ashes, such as glassy phase and metakaoline, will be able to react with $Ca(OH)_2$ as a pozzolanic material. The glassy phase contains SiO_2, Al_2O_3 and CaO as major oxides and it has a similar composition as blast furnace slag. The metakaoline actively reacts under the hydrothermal condition [13]. In addition, these amorphous components accelerate the crystallization of C–S–H gel to tobermorite [14] and contrib-

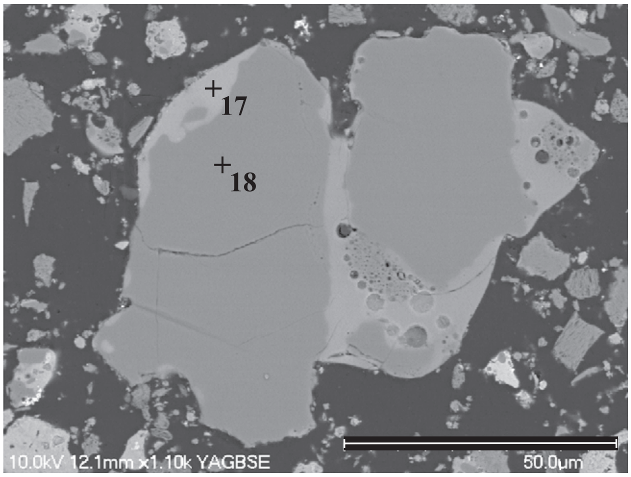

analysis point	17	18
SiO_2	60.1	92.0
Al_2O_3	14.8	3.3
CaO	22.4	2.7
MgO	0.1	-
Na_2O	0.1	0.3
TiO_2	1.3	-
SO_3	1.3	1.6

(mass%)

17: glassy phase
18: quartz

Fig. 7. SEM photograph and EDX results for quartz and glassy phase in the PFBC ash from Wakamatsu.

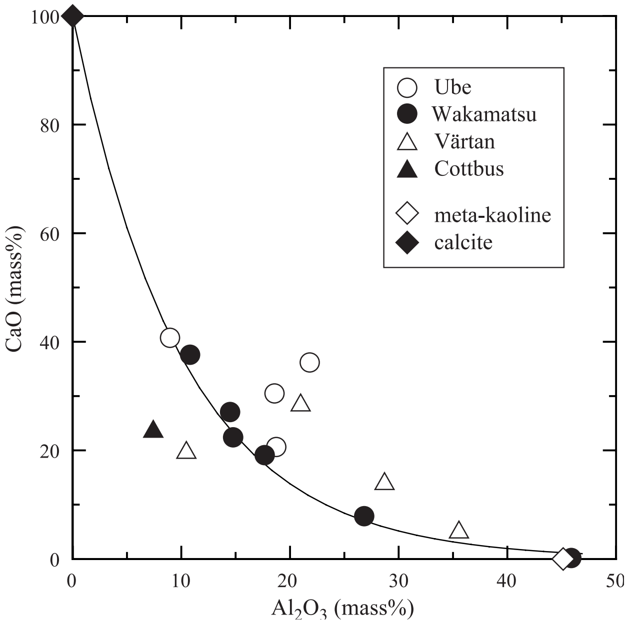

Fig. 8. Relationship between Al_2O_3 and CaO concentration analyzed by EDX on the glassy phase.

ute to the formation of hydrogarnet [13,15] because of the presence of Al_2O_3 in the amorphous phases. Therefore, the advantage as reduction of processing time is expected in the manufacturing process of a product using the PFBC ashes.

4. Conclusions

The electron microscopy and chemical analysis by EDX was applied in microscopic and mineralogical characterization of each mineral in PFBC ashes. A summary of our findings is as follows:

(1) The high-purity limestone, which was used in Japanese PFBC plants, resulted in the formation of both hydroxyl ellestadite ($Ca_{10}(SiO_4)_3(SO_4)_3(OH)_2$) and anhydrite ($CaSO_4$), while dolomite-rich limestone, which was used in European PFBC plants, resulted in the formation of anhydrite.

(2) PFBC ashes had hydroxyl ellestadite particles as the independent particle or the rim of limestone particle. This suggested that the hydroxyl ellestadite formed as rims around limestone particles and then it formed independent particles as a result of exfoliation by hard agitation in the fluidized bed. Under high magnification, it was observed that hydroxyl ellestadite was mingled with anhydrite in the size of several micrometers.

(3) Al_2O_3 concentration in glassy phase is inversely proportional to the CaO concentration. This suggests that the glassy phase was formed as a result of reaction in the mixture of metakaoline and calcite.

(4) By using PFBC ashes with hydroxyl ellestadite as a raw material in hydrothermal technology, the formation of highly crystalline tobermorite and the improvement of strength and durability for shrinkage with the carbonation will be achieved. Since the amorphous phases, such as glassy phase and metakaoline, accelerate the crystallization of C–S–H gel to tobermorite, the reduction of processing time is expected in the manufacture process.

Acknowledgements

We wish to express our gratitude to Chugoku Electric Power, Electric Power Development, Hokkaido Electric Power, Kyushu Electric Power, Birka Energi, Stadwerke-Cottbus Kommunalfinanz Gruppe and ABB Carbon for providing us with the PFBC ashes.

References

[1] P. Almhem, J. Lofe, PFBC power plants: a competitive alternative, Power-Gen 96 Book 3 C 7 9 Gener Trends, 1996, pp. 169-195, Orland.

[2] J.F. Stubington, A.L.T. Wang, Y. Cui, Understanding the behaviour of Australian black coals in pressurised fluidized bed combustion, Proceedings of the 15th International Conference on Fluidized Bed Combustion, American Society of Mechanical Engineers, New York, 1999, No. FBC99-0005.

[3] C. Nilsson, L.B. Clarke, PFBC Residues—Characteristics, Disposal and Utilisation, EA Coal Research, London, 1994.

[4] S. Orchard, Technical Coal Research—Disposal and Utilisation of Ash Residues from Pressurised Fluidised Bed Combustion, Commission of the European Communities, Brussels, 1991.

[5] R. Kondo, Kinetics on hydrothermal reaction between lime and silica, Proceedings of International Symposium on Autoclaved Calcium Silicate Building Products, Society of Chemical Industry, London, 1965, pp. 92–97.

[6] T. Yamamoto, H. Ishida, T. Mitsuda, Some properties of autoclaved calcium silicate materials using waste tile: Influence of SiO_2 sources, in: E.M. Gartner, H. Uchikawa (Eds.), Ceramic Transactions, Vol. 40, Cement Technology, American Ceramic Society, Westerville, 1994, pp. 223–230.

[7] H. Maenami, T. Yamamoto, H. Ishida, T. Mitsuda, Hydrothermally prepared inorganic siliceous wastes: hydrothermal reaction of calcareous and steatite ceramic tile wastes, in: V. Jain, D. Peeler (Eds.), Ceramic Transactions, Vol. 72, Environmental Issues and Waste Management Technologies in the Ceramic and Nuclear Industries II, American Ceramic Society, Westerville, 1996, pp. 375–384.

[8] K.P. Yrjas, K. Iisa, M. Hupa, Sulphur absorption capacity of different limestones and dolomites under pressurized combustion conditions, Proceedings of the 12th International Conference on Fluidized Bed Combustion, American Society of Mechanical Engineers, New York, 1993, pp. 265–271.

[9] C. Tullin, G. Nyman, S. Ghardashkhani, Direct sulfation of $CaCO_3$: the influence of CO_2 partial pressure, Energy Fuels 7 (1993) 512–519.

[10] H.F.W. Taylor, Cement Chemistry, Academic Press, New York, 1990.

[11] A.E. Moore, The sequence of compound formation in Portland cement rotary kilns. 2, Cem. Technol. 7 (85) (1976) 134–138.

[12] M. Sakiyama, Y. Oshio, T. Mitsuda, Influence of gypsum on the

hydrothermal reaction of lime–quartz system and on the strength of autoclaved calcium silicate product, J. Soc. Inorg. Mater. Jpn. 7 (2000) 685–691.

[13] D.S. Klimesch, A. Ray, Hydrogarnet formation during autoclaving at 180 °C in unstirred metakaolin–lime–quartz slurries, Cem. Concr. Res. 28 (8) (1998) 1109–1117.

[14] M. Sakiyama, T. Mitsuda, Hydrothermal reaction between C–S–H and kaolinite for the formation of tobermorite at 180 °C, Cem. Concr. Res. 7 (1977) 681–685.

[15] H. Maenami, O. Watanabe, H. Ishida, T. Mitsuda, Hydrothermal solidification of kaolinite–quartz–lime mixture, J. Am. Ceram. Soc. 83 (7) (2000) 1739–1744.